EFFECTS OF IMPINGING JET FLOW ON PLATELETS ADHESION BY COMPUTATIONAL FLUID DYNAMICS (CFD) ANALYSIS WITH CONSIDERATION OF PARTICLE MOTION FOR PREDICTING THROMBUS FORMATION

Shohei Nakata, Yuko Miyamura and Masaaki Tamagawa

Graduate School of Life Science and Systems Engineering
Kyushu Institute of Technology
2-4 Hibikino, Wakamatsu-ku, Kitakyushu, Fukuoka 808-0196, Japan
tama@life.kyutech.ac.jp

Abstract. *To establish the prediction method of thrombus formation on the wall by computational fluid dynamics (CFD), it is very important to find out the effects of flow field on platelet adhesion on the wall. In this paper, the particle motions on impinging jet flow which has the stagnation point were analyzed, and the adhered particles on the wall were also analyzed. Especially, discrete particles by using the impinging jet flow that Affeld used for the platelet adhesion experiment were analyzed, and the adhesion mechanism of particles simulating platelets was investigated by CFD. This adhesion mechanism is corresponded to starting point for thrombus formation on shear flow. After analyzing three-dimensional flow field particle motions by using fundamental equations on the impinging jet flow, the platelet motions can be obtained. From the result of CFD comparing with experiment, it was concluded that the platelet motion was able to be simulated on the impinging jet flow by using particle tracking method with consideration of density difference. It was also concluded that predicted adhered distribution did not agree well with experimental result even though the tendency of distribution of adhered platelet could be obtained. Further investigation and trials for this validation will be needed to establish the prediction method.*
Keywords: Impinging jet flow, Thrombus formation, Particle motion, Platelet adhesion

1. **Introduction.** Recently design and development of medical fluidics including artificial hearts, artificial valves and stent have been world-widely investigated, but the hemolysis and the thrombus formation occurring in these devices are still now serious problems [1-7]. For designers of these medical fluidics, CFD (computational fluid dynamics) is a powerful tool to develop them. However, it is still now difficult to predict the thrombus formation in these devices by CFD analysis.

In our previous investigation [8-10], to find out the correlation between flow field and thrombus formation on shear flows in the orifice pipe and Couette flows, visualization of thrombus formation and CFD analysis were done. In the previous CFD analysis, flow analysis on the pipe orifice flow was carried out and the flow field data was obtained in detail. As a result, the possibility of thrombus formation and platelet adhesion near the reattachment point of the orifice pipe was suggested. However, it was difficult to find out the correlation between flow field and thrombus formation directly by comparing with the visualization of thrombus formation. Considering about this problem, there is one possibility to investigate the platelet adhesion on the device wall for detecting because the thrombus is generating from the adhered platelets by shear flow. However, effects of platelets adhesion on the thrombus formation have not been elucidated yet.

For this adhesion problem, Affeld [11] has already focused on the impinging jet flow as a simple model of shear flow in the medical fluidics, and they have observed the platelet adhesion on the jet wall. In their work, after conducting fundamental experiments on platelet adhesion on the wall of impinging flow, they obtained particle distribution flown from the inlet, and also obtained 2 dimensional position of platelet adhesion on the wall from top view. They also concluded that evaluation of platelet adhesion could be done from the distribution of adhered platelets and the shear rate distribution on the impinging wall. Therefore, it is necessary to investigate the tendency of adhered particles on the wall by particle analysis of CFD using the same impinging jet flow. However, the mechanism of adhesion of platelets on the walls by the flow, and the effects of wall shear stress distribution on the thrombus are still now unknown.

For understanding these phenomena, Lagrangian approach is powerful tool for evaluating each particle and total particles compared with Eulerian approach. Giersiepen et al. [12] investigated the hemolysis evaluation by using particles as red blood cells. This particle tracking method is a very useful approach for evaluation of damage accumulation of particles. Platelet activation for thrombus formation is caused by platelet stimulation, and then this approach is applicable to predicting thrombus formation by evaluating of accumulation of platelets stimulation. From the engineering point of view, it is necessary for prediction of trigger points of thrombus formation to develop and establish the evaluation method by this particle tracking approach.

In this investigation, the particle motions on impinging jet flow which has the stagnation point are analyzed, and the particle adhesion on the wall is also analyzed. Especially, discrete particles by using the impinging jet flow that Affeld used for the platelet adhesion experiment are analyzed where the stagnation point occurs, and the adhesion mechanism of particles simulating platelets is investigated by CFD. This adhesion mechanism is corresponded to thrombus formation on shear flow. It is expected to predict the thrombus formation more precisely than present computation by considering this aggregation process.

In this paper, the computational objects and computational methods of three-dimensional impinging jet flow are described in Section 2, and the results and related matters are discussed using computer simulations of impinging jet flow and particle motions in Section 3. And the result of distribution of adhered platelets on the wall by three-dimensional CFD analysis is compared with that of distribution by experiments. In addition, effects of density difference between particle and fluid are also confirmed and discussed. In Section 4, concluding remarks are described.

2. Objects and Method.

2.1. **Computational objects.** In this calculation, an axially symmetric three-dimensional geometry is presented. The diameter of inflow port D_1 is 0.67 [mm], the distance from top to the bottom surface h is 0.40 [mm], and the diameter of bottom surface D_2 is 2.0 [mm] as shown in Figure 1. These dimensions are set to be the same as the model of Affeld [11].

2.2. **Computational method.** As for computational method for the particle tracking method, there are two parts including Eulerian method and Lagragian method. Impinging jet flow is analyzed by Eulerian method, and particle is analyzed by Lagragian method alternatively.

2.2.1. *Fundamental equations for flow.* Regarding as fundamental equations of the flow, the following continuity equations, Navier-Stokes equations are used as follows:
 (1) Continuity equation

$$\nabla \cdot \mathbf{v} = 0 \tag{1}$$

(2) Navier-Stokes equation with turbulence

$$\frac{\partial \mathbf{v}}{\partial t} + (\mathbf{v} \cdot \nabla) \mathbf{v} = -\frac{1}{\rho}\nabla p + \nu \Delta \mathbf{v} + \mathbf{F} \tag{2}$$

where $\mathbf{v}$ indicates velocity vector $\mathbf{v}(u, v, w)$, ρ is fluid density, p is pressure, ν is dynamic viscosity, and $\mathbf{F}$ is interaction force between particle and fluid flow, which are derived from particle motions.
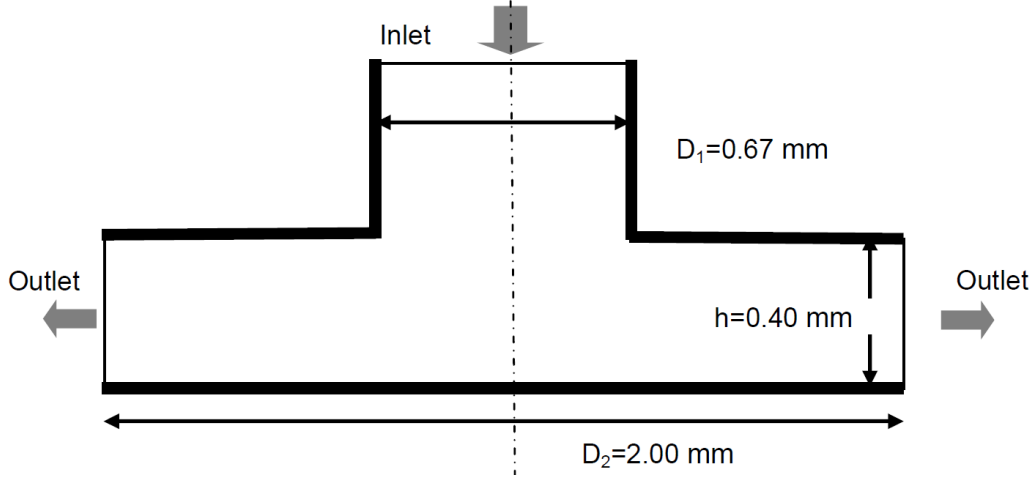

FIGURE 1. Geometries of impinging jet flow

2.2.2. *Equation of motion of particles.* On the impinging jet flow in previous subsection, the discrete particles are flown and analyzed for their motion to trace the platelet motions. Here the equation of motion of the particles is described. When the position of each i-th particle is $\mathbf{x}_{p,i}$ and the particle velocity is $\mathbf{u}_{p,i}$, the equation of motion of the particle is expressed as follows:

$$\frac{d\mathbf{x}_{p,i}}{dt} = \mathbf{u}_{p,i} \tag{3}$$

$$m_p \frac{d\mathbf{v}_{p,i}}{dt} = \mathbf{F}_i \tag{4}$$

$$\mathbf{F}_i = \mathbf{F}_{drag,i} + \mathbf{F}_{gravity,i} + \mathbf{F}_{ext,i} \tag{5}$$

where $\mathbf{F}_i$ is F represents all the body forces and surface forces acting on the i-th particle. $\mathbf{F}_{ext,i}$ is a force applied elsewhere and virtual masses, and in this investigation this term is assumed to be 0. By using (4) and (5), the equilibrium of the inertia of the particle and the force acting on the particle is described as follows:

$$\frac{d\mathbf{v}_{p,i}}{dt} = f_D (\mathbf{v} - \mathbf{v}_{p,i}) + \mathbf{G}\frac{\rho_p - \rho}{\rho_p} \tag{6}$$

where $\mathbf{v}$ is the velocity of the flow field, ρ is the density of the fluid, ρ_p is the density of the particle, and $\mathbf{G}$ is gravity acceleration. f_D is the coefficient per unit particle mass, and shown as follows:

$$f_D = \frac{18\mu}{\rho_p d_p^2} \frac{C_D Re_p}{24} \tag{7}$$

where μ is the molecular viscosity of the fluid, and d_p is the diameter of the particle. Re_p is the particle Reynolds number, and it can be obtained from the relative speed with the fluid as follows:

$$Re_p = \rho d_p \frac{|\mathbf{v} - \mathbf{v}_{p,i}|}{\mu} \tag{8}$$

C_D is the drag coefficient, and in this investigation it is represented as follows:

$$C_D = a_1 + \frac{a_2}{Re_p} + \frac{a_3}{Re_p^2} \tag{9}$$

Each coefficient a_i is determined from the value range of Re_p and is shown in Table 1. This is Morsi and Alexander's empirical formula [13], which can be used with a wide range of Reynolds numbers.

TABLE 1. Coefficient parameters for Reynolds number

	a_1	a_2	a_3
$0 < Re_p < 0.1$	0.00	24.00	0.00
$0.1 < Re_p < 1.0$	3.69	22.73	0.09
$1.0 < Re_p < 10.0$	1.22	29.17	-3.89
$10.0 < Re_p < 100.0$	0.62	46.50	-116.67
$100.0 < Re_p < 1000.0$	0.36	98.33	-2778

2.3. **Pre-processing issues.** As for the flow analysis in the three-dimensional flow, the thermo-fluid dynamics code (FLUENT, ANSYS 17.2) is used. Figure 2 shows typical mesh of three-dimensional flow, and the computational mesh generated by ICEM CFD (including ANSYS 17.2) is tetrahedral type. For the mesh refinement, total number of element is approximately 450,000 and it was validated to be enough resolution for the Reynolds number in this investigation.
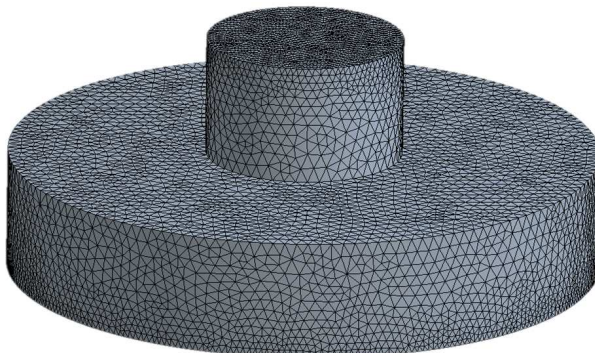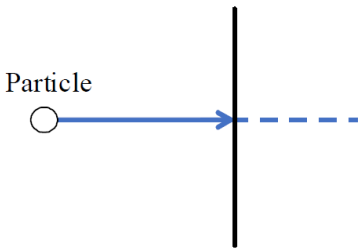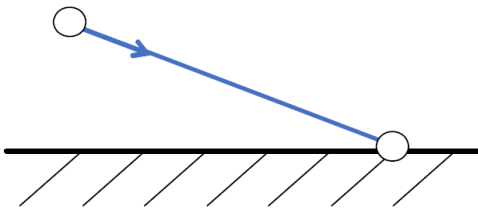

FIGURE 2. Three-dimensional FEM mesh for CFD analysis

2.4. **General boundary conditions.** As boundary conditions, inlet flow rate Q is 5.55 [m^3/s], which was the same as that of Affeld's experiment. The average flow rate U_{in} is 15.8 [mm/s], fluid density ρ is 1000 [kg/m^3], and Reynolds number Re is 9.5. No-slip condition is given to the wall surface, and pressure p is given to be $= 0$ [Pa] at the outlet part. Also, assuming that plasma water flows, viscosity μ is set up to be 1.3×10^{-3} [Pa · s]. Because the Reynolds number is smaller than the threshold Reynolds number, the flow can be dealt as laminar flow. For coupling analysis of discrete particle motion together with fluid flow, the diameter of the particle d_p is 3.0×10^{-6} [m] and the density ρ_p is 1050 [kg/m^3] based on the physical properties of the platelet. The time step is set up to be 0.0005 [s], and total computational time is 200 [s].

2.5. **Boundary condition for particle motions.** As boundary conditions related to particles, there are two boundary conditions such as 'Escape' and 'Trap' on the wall surface at the inlet or outlet boundary of the flow. In case of Escape condition, calculation of the particle is completed when it reaches the inlet or outlet boundary conditions. In case of Trap condition, the particle loses momentum when it comes in contact with wall.

TABLE 2. Boundary conditions for particle motions

Location	Particle status for boundary
Inlet or Outlet	Escape Particle
Wall	Trap Particle

The typical image for each boundary condition is shown in Table 2. In addition to these boundary conditions, as for adhered particles, the height of one cell of the mesh from the bottom is taken as threshold length to adhere particles on the wall.

3. **Results and Discussions.** Figure 3 shows the trajectory traces of particles from the side view. From this figure it can be found that this flow is approximately axisymmetric and has a stagnation point at the bottom center. After particle collision with the bottom surface, some particles adhere according to the boundary condition of the bottom wall.
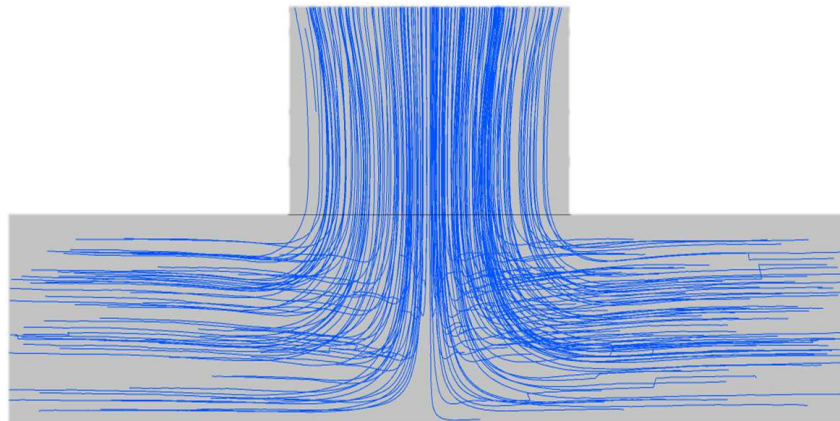

FIGURE 3. Path-line for the flow field

By the way, Figure 4 shows typical adhered platelet distribution on the wall on the microscope in Affeld's experiment. From this figure, it is clearly found that there are not so many particles at the center (stagnation point). In this figure, the scale is also shown, and it is used for obtaining probability density function of platelets on the wall.

Figure 5 shows time procedure of three-dimensional particle distribution in impingement flow by particle tracking. From this figure, it is found that particles move downward from the inlet port and some of them collide with the bottom walls. It is also found that the particle distribution is not uniform due to 3-dimensional effects as same as experimental results in Figure 4. Then it is necessary for comparing CFD with experiment to arrange probability density function (PDF) of particle number by averaging along the
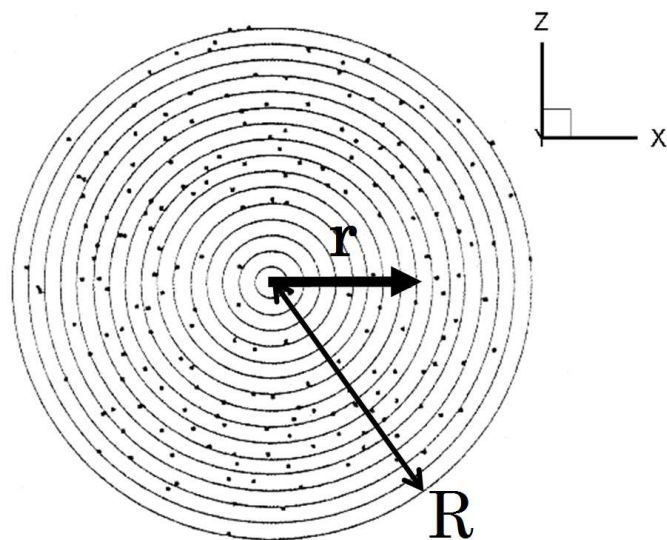
FIGURE 4. Adhered platelet distribution on the wall by the experiment [11]

$t = 0.01$ [s]

$t = 0.05$ [s]

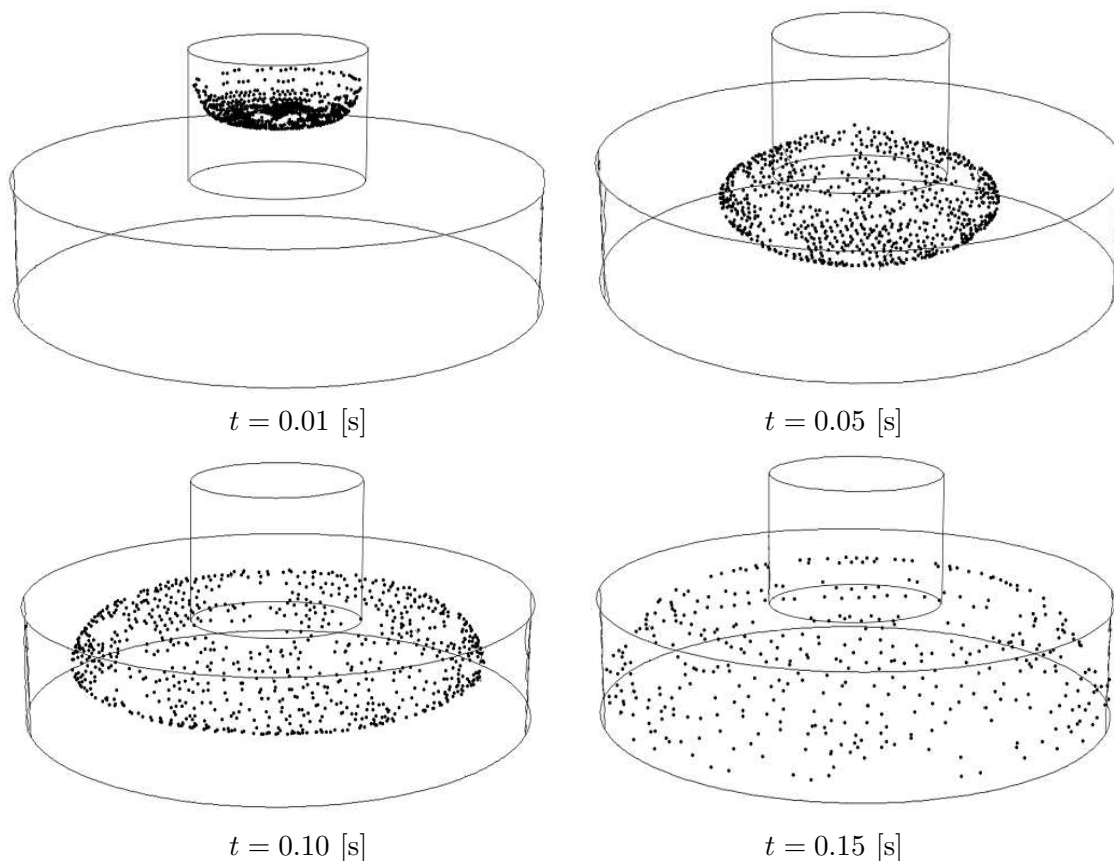$t = 0.10$ [s]

$t = 0.15$ [s]

FIGURE 5. Time procedure of three-dimensional particle distribution in impingement flow

tangential direction. Figure 6 shows arranged distribution of adhered normalized particle numbers (PDF) on the bottom wall along the radial direction in case of CFD and experiment.

In this figure, the horizontal axis shows the ratio of the entrance radius r to the bottom surface radius R, and the vertical axis shows normalized particle numbers (PDF). Although the width of distribution between Figure 6(a) and Figure 6(b) is different, there is similar tendency of decaying the number of adhered particles with time procedure.
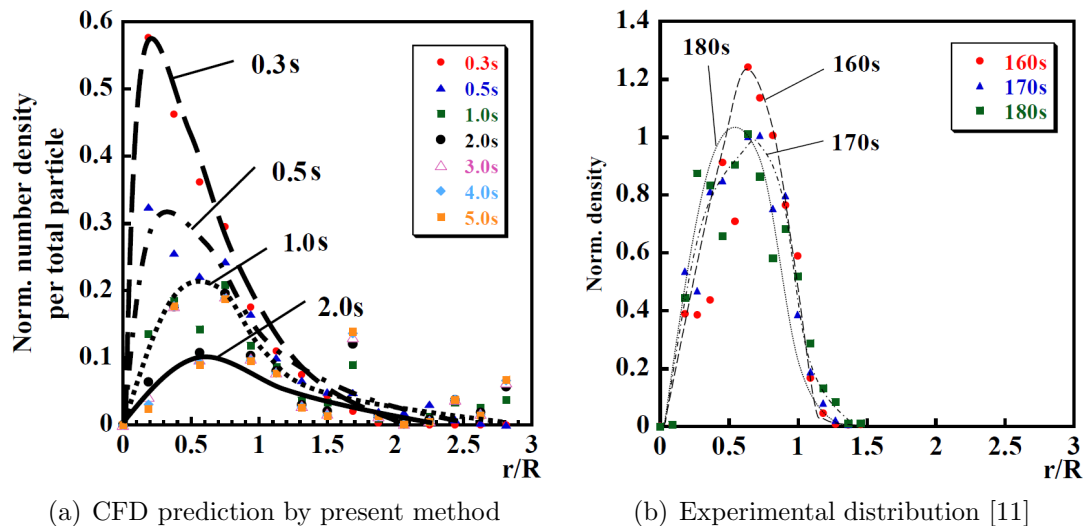
(a) CFD prediction by present method   (b) Experimental distribution [11]

FIGURE 6. Distribution of normalized number density (probability density function) along radial direction r

However, there is large difference of time scale between CFD and experiment. The reason why the time scale is different is considered to be due to the difference of adhesion force between actual platelets and model platelets. Further investigation about this matter is needed to confirm this difference by arranging the adhesion force or adhered length defined at 'Trap' boundary conditions.

4. **Conclusions.** To investigate effects of flow field on platelet adhesion on shear flow, the effects of platelet adhesion on the wall surface on thrombus formation were investigated by analyzing three-dimensional flow field on the impinging jet flow. The following issues are concluded as follows.

(1) By using particle tracking method with consideration of density difference between particle and fluid, the platelet motion was able to be simulated on the impinging jet flow.

(2) As for adhesion process, predicted adhered distribution did not agree well with experimental result even though the tendency of distribution of adhered platelet could be obtained. However, this tendency will increase the accuracy of the prediction at all.

It is expected to predict the thrombus formation more precisely than present computation by considering these results. Further investigation and trials for this validation will be needed to establish the prediction method by finding out adhesion force of platelet with the wall.

REFERENCES

[1] T. Akamatsu, T. Tsukiya, K. Nishimura, C. H. Park and T. Nakazeki, Recent studies of the centrifugal blood pump with a magnetically suspended impeller, *Artificial Organs*, vol.19, no.7, pp.631-634, 1995.

[2] U. Morbiducci, R. Ponzini, M. Nobili, D. Massai, F. M. Montevecchi, D. Bluestein and A. Redaelli, Blood damage safety of prosthetic heart valves, shear-induced platelet activation and local flow dynamics: A fluid-structure interaction approach, *Journal of Biomechanics*, vol.42, no.12, pp.1952-1960, 2009.

[3] F. M. Susin, S. Espa, R. Toninato, S. Fortini and G. Querzoli, Integrated strategy for in vitro characterization of a bileaflet mechanical aortic valve, *Biomed. Eng. Online*, vol.16, no.1, p.29, 2017.

[4] S. C. Shadden and A. Arzani, Lagrangian postprocessing of computational hemodynamics, *Ann. Biomed. Eng.*, vol.43, no.1, pp.41-58, 2015.

[5] R. A. Malinauskas, P. Hariharan, S. W. Day, L. H. Herbertson, M. Buesen, U. Steinseifer, K. I. Aycock, B. C. Good, S. Deutsch, K. B. Manning and B. A. Craven, FDA benchmark medical device flow models for CFD validation, *ASAIO J.*, vol.63, no.2, pp.150-160, 2017.

[6] Z. Xu, J. Lioi, J. Mu, M. M. Kamocka, X. Liu, D. Z. Chen, E. D. Rosen and M. Alber, A multiscale model of venous thrombus formation with surface-mediated control of blood coagulation cascade, *Biophysical Journal*, vol.98, pp.1723-1732, 2010.

[7] G. Moiseyev, S. Givli and P. Z. Bar-Yoseph, Fibrin polymerization in blood coagulation – A statistical model, *Journal of Biomechanics*, vol.46, pp.26-30, 2013.

[8] Y. Yi, M. Tamagawa and W. Shi, Prediction of thrombus formation on the wall by high shear pate on couette and orifice blood flows, *Journal of Medical Imaging and Health Informatics*, vol.7, no.1, pp.79-84, 2017.

[9] C. Hirayama, Y. Miyamura and M. Tamagawa, Effects of flow asymmetricity on thrombus formation and hemolysis properties in the pipe orifice flow by CFD analysis, *ICIC Express Letters, Part B: Applications*, vol.9, no.7, pp.673-680, 2018.

[10] Y. Yi and M. Tamagawa, Simulation of platelet aggregation on the wall of orifice flow by dissipative particle dynamics accelerated by OpenMP, *ICIC Express Letters, Part B: Applications*, vol.9, no.7, pp.665-672, 2018.

[11] K. Affeld, Fluid mechanics of the stagnation point flow chamber and its platelet deposition, *Artificial Organs*, vol.19, no.7, pp.597-602, 1995.

[12] M. Giersiepen, L. J. Wurzinger, R. Opitz and H. Reul, Estimation of shear stress related blood damage in heart valve prostheses – In vitro comparison of 25 aortic valves, *International Journal of Artificial Organs*, vol.13, no.5, pp.300-306, 1990.

[13] S. A. Morsi and A. J. Alexander, An investigation of particle trajectories in two-phase flow systems, *Journal of Fluid Mechanics*, vol.55, no.2, pp.193-208, 1972.